# Zn(II)-, Al(III)-, and Cu(II)-Catalyzed Decarboxylation of 2-Oxalopropionic Acid

## Gregory Kubala[†] and Arthur E. Martell*

*Contribution from the Department of Chemistry, Texas A&M University, College Station, Texas 77843. Received January 18, 1982*

**Abstract:** Distributions of species formed by the coordination of 2-oxalopropionic acid by Zn(II), Al(III), and Cu(II) ions are presented, and kinetics of decarboxylation are discussed in terms of the species present in solution. Studies of initial rates of metal ion catalyzed decarboxylation of 2-oxalopropionic acid ($H_2L$) show dependence on the degree of formation of the metal chelate (ML). Rate constants ($k_{ML}$) for the decarboxylation of ZnL, CuL, and $AlL^+$ were found to be $18.2 \times 10^{-3}$ $s^{-1}$, $21.0 \times 10^{-3}$ $s^{-1}$, and $9.51 \times 10^{-3}$ $s^{-1}$, respectively. The equilibrium constants for ML(keto) $\rightleftharpoons$ ML(enol) were evaluated for the Zn(II) and Al(III) systems and rate constants ($k^K_{ML}$) for the decarboxylation of the active keto forms of the Zn(II) and Al(III) chelates were found to be $31 \times 10^{-3}$ $s^{-1}$ and $79 \times 10^{-3}$ $s^{-1}$, respectively. The decarboxylation rate constant for the 2:1 Al(III) chelate, $AlL_2^-$, was determined to be $33.5 \times 10^{-3}$ $s^{-1}$. The keto–enol equilibrium constant $[AlL_2^-(enol)]/[AlL_2^-(keto)]$ was evaluated, and the decarboxylation rate constant of $AlL_2^-(keto)$ was calculated as $43 \times 10^{-3}$ $s^{-1}$.

Metal ion catalyzed decarboxylation of $\beta$-carboxy $\alpha$-keto carboxylic acids has been studied extensively[1-17] and is of considerable interest because of its importance in metabolic reactions of biological systems. In addition to the studies of metal ion catalysis, studies of spontaneous[1-3,6,18-21] and enzymatic[2,22,23] decarboxylation have been reported as well as investigations of enolization,[24-26] dehydration,[24,26] and hydration.[26] Substrates that have been involved in these studies are oxaloacetic acid (OAA), dimethyloxaloacetic acid (DMOAA), fluorooxaloacetic acid (FOAA), and 2-oxalopropionic acid (3-methyl-2-oxobutanedioic acid, OPA). Decarboxylation of these substrates results in the formation of pyruvic, $\alpha$-ketoisovaleric, fluoropyruvic, and $\alpha$-ketobutyric (AKBA) acids, respectively.

Sakkab and Martell[18] introduced 2-oxalopropionic acid as a substrate for decarboxylation because the $\beta$-methyl group of OPA provides a direct and effective NMR probe during the decarboxylation process. Also, OPA has the ability to enolize and in this respect is a better model for OAA than a previously studied analogue, DMOAA. Initial studies[18,19,27] on the decarboxylation of OPA, ketonization of the enolic AKBA intermediate, enolization of OPA, and the determination of proton association and metal ion ($Zn^{2+}$, $Cu^{2+}$, $Al^{3+}$) formation constants have been carried out in this laboratory. The present studies involve the rates of metal ion catalyzed decarboxylation of OPA, while the next step in the ongoing work is the investigation of pyridoxamine catalysis of the decarboxylation reaction. The vitamin $B_6$ catalyzed systems are considered important since the Schiff bases of OAA and its analogues with pyridoxamine are models for the probable intermediates in the corresponding enzyme-catalyzed processes.

Steinberger and Westheimer[1] made a fundamental advance in metal ion catalysis of $\alpha$-keto diacids in which the second carboxyl function is bound to the $\beta$-carbon atom by demonstrating that the five-membered chelate ring involving the $\alpha$-keto oxygen is the active catalytic species in OAA–metal ion systems. Nearly 20 years later Reyes-Zamora and Tsai[28] measured NMR spectra of europium(III) oxaloacetates indicating that the main species formed has a five-membered chelate ring. No evidence was found for the formation of larger chelate rings. Covey and Leussing[9] found that the five-membered form of the Zn(II)–OAA chelate predominates in solution under their experimental conditions but suggested that 10–20% of the coordinated ligand may exist as the seven-membered chelate ring in which both carboxyl functions are directly coordinated to the Zn(II). Kubala and Martell[27] proposed on the basis of potentiometric studies that the five-membered chelate rings (1a, 1b) are the major forms in OPA–metal ion systems but that the six-membered metal chelate rings

**Scheme I**
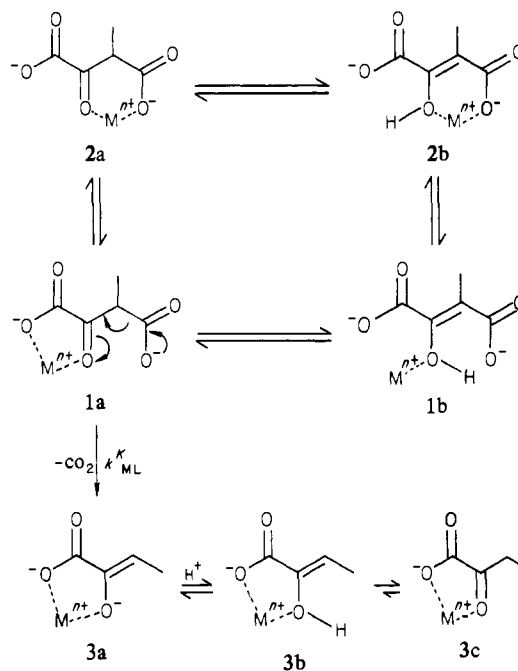


(2a, 2b) contribute as much as 15% of the total metal species present.

(1) Steinberger, R.; Westheimer, F. H. *J. Am. Chem. Soc.* **1951**, *73*, 429.
(2) Krebs, H. *Biochem. J.* **1942**, *36*, 303.
(3) Pedersen, K. J. *Acta Chem. Scand.* **1952**, *6*, 285.
(4) Kosicki, G. W.; Lipovac, S. N. *Can. J. Chem.* **1964**, *42*, 403.
(5) Dummel, R. J.; Berry, M. H.; Kun, E. *Mol. Pharmacol.* **1971**, *7*, 367.
(6) Steinberger, R.; Westheimer, F. H. *J. Am. Chem. Soc.* **1949**, *71*, 4158.
(7) Gelles, E.; Salama, A. *J. Chem. Soc.* **1958**, 3683, 3689.
(8) Speck, J. F. *J. Biol. Chem.* **1949**, *178*, 315.
(9) Covey, W. D.; Leussing, D. L. *J. Am. Chem. Soc.* **1974**, *96*, 3860.
(10) Raghavan, N. V.; Leussing, D. L. *J. Am. Chem. Soc.* **1976**, *98*, 723.
(11) Rund, J. V.; Claus, K. G. *J. Am. Chem. Soc.* **1967**, *89*, 2256.
(12) Duc, G.; Thomas, G. *Bull. Soc. Chim. Fr.* **1972**, 4439.
(13) Ito, H.; Kobayashi, H.; Nomiya, J. *J. Chem. Soc., Faraday Trans. 1* **1973**, *69*, 113.
(14) Munakata, M.; Matsui, M.; Tabushi, M.; Shigematsu, T. *Bull. Chem. Soc. Jpn.* **1970**, *43*, 114.
(15) Bamann, E.; Sethi, V. S. *Arch. Pharm. (Weinheim, Ger.)* **1968**, *301*, 78.
(16) Claus, G. C.; Rund, J. V. *Inorg. Chem.* **1969**, *8*, 59.
(17) Gelles, E.; Hay, R. W. *J. Chem. Soc.* **1957**, 3673.
(18) Sakkab, N. Y.; Martell, A. E. *J. Am. Chem. Soc.* **1976**, *98*, 5285.
(19) Kubala, G.; Martell, A. *J. Am. Chem. Soc.* **1981**, *103*, 7609.

† Abstracted in part from a dissertation submitted by Gregory Kubala to the faculty of Texas A&M University in partial fulfillment of the requirements for the degree of Doctor of Philosophy.

The primary goal of the present investigation is to carry out kinetic studies to probe the proposed mechanism for metal ion catalyzed decarboxylation presented in Scheme I. The pH dependence of the decomposition of OPA in the presence of either Zn(II), Cu(II), or Al(III), the corresponding proton association constants, and metal chelate stability constants are employed to calculate the rate constants for the decarboxylation of the metal chelates ($k_{ML}$) present in solution from the observed rate constants ($k_{obsd}$) of metal ion catalysis. Also, where possible, the specific rate constants ($k^K_{ML}$) for the decarboxylation of the active keto forms of the OPA–metal ion complexes are determined. This is the first report of values for $k_{ML}$ and $k^K_{ML}$ in OPA–metal ion systems. Also, very few analogous rate constants have been reported for other $\beta$-carboxy $\alpha$-keto carboxylic acid–metal ion systems. Previous studies of this nature are limited to reports of the aqueous OAA–Cu(II) and OAA–Zn(II) systems by Leussing et al.[9,10]

## Experimental Section

**Materials.** 2-Oxalopropionic acid was prepared by acid hydrolysis of diethyl oxalopropionate, purchased from Aldrich Chemical Co., according to the procedure described by Kubala and Martell.[19] Stock solutions of reagent grade Al(III), Zn(II), and Cu(II) were prepared from the metal chlorides with doubly distilled water. The exact concentrations were determined by titration with standard EDTA[29] solutions and were approximately $1.6 \times 10^{-3}$ M. The Al(III) stock solution was stored at acidic pH to prevent the formation of appreciable amounts of polynuclear aluminum hydroxide species that are involved in slow equilibrium with mononuclear aquo Al(III) and hydroxide ion. The prevention of polynuclear species was necessary since rapid equilibrium between metal chelate and free metal ion and substrate is required for analysis of the kinetic data. The stock solution of OPA prepared with double distilled water was stored at 0 °C and brought to 25.0 °C just before each kinetic run. The concentration of OPA stock solutions were about $1.60 \times 10^{-3}$ M and were determined by titration with standardized aqueous KOH. The supporting electrolyte was potassium chloride and was obtained as reagent grade material. The pH of the reaction mixtures was controlled by the addition of aqueous HCl or a carbonate-free solution of KOH prepared from Dilut-it (R) ampules.

**Measurements.** The pH values were obtained with a Beckman research pH meter fitted with Fisher reference and universal glass electrodes. The meter was standardized so as to read hydrogen ion concentration directly.

Kinetic data were obtained by monitoring the maximum absorption in the ultraviolet region for OPA, which occurs at 260 nm. The absorptivity was measured on a Cary-14 recording spectrophotometer with a quartz cell having a 1.000-cm path length. The apparent extinction coefficients at 260 nm for OPA–metal ion systems at various hydrogen ion concentrations were determined from initial absorption measurements taken within 30 s of the time of mixing of OPA and metal ion solutions. The reaction solutions were measured in an experimental setup that allowed simultaneous ultraviolet and pH measurements. The temperatures of the reaction vessel and quartz cell were maintained at $25.0 \pm 0.1$ °C with a Haake constant-temperature bath. The ionic strength of the reaction solutions was maintained at 0.100 M with KCl. The OPA, Al$^{3+}$, and Cu$^{2+}$ concentrations were $1.000 \times 10^{-4}$ M and the OPA and Zn$^{2+}$ concentrations were $5.00 \times 10^{-4}$ M.

Kinetic measurements were conducted on unbuffered solutions in order to eliminate the catalytic effects buffers may have on the rate of decarboxylation or on the concentrations of free metal ion. The absence of buffers allows the accurate calculation of specific rate constants of decarboxylation of the various metal chelate species. The absence of buffering agents in the system resulted in some drift of the pH in the weakly acidic regions during the course of the reaction, but error in kinetic values due to this drift was minimized by using initial rates. All measurements were taken before the shift in pH became significant. Measurements above pH 6 were not taken since CO$_2$ absorption becomes

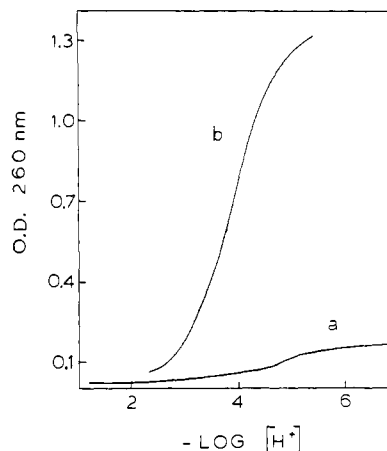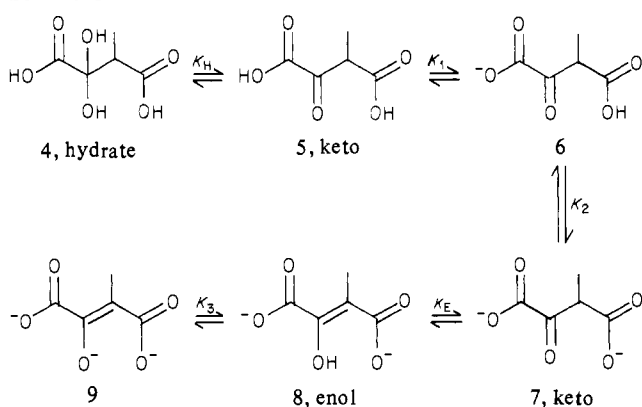(20) Gelles, E. *J. Chem. Soc.* **1956**, 4736.
(21) Ochoa, S. *J. Biol. Chem.* **1948**, *174*, 115.
(22) Krampitz, L. D.; Werkman, C. W. *Biochem. J.* **1941**, *35*, 595.
(23) O'Leary, M. H.; Piazza, G. *J. Biochem.* **1981**, *20*, 2743.
(24) Emly, M.; Leussing, D. L. *J. Am. Chem. Soc.* **1981**, *103*, 628.
(25) Bruice, P. J.; Bruice, T. C. *J. Am. Chem. Soc.* **1978**, *100*, 4793.
(26) Pogson, E. I.; Wolfe, R. G. *Biochem. Biophys. Res. Commun.* **1972**, *46*, 1048.
(27) Kubala, G.; Martell, A. E. *Inorg. Chem.*, in press.
(28) Reyes-Zamora, C.; Tsai, C. S. *J. Chem. Soc. D* **1971**, 1047.
(29) Schwarzenbach, G.; Flaschka, H. "Complexometric Titrations", 2nd English ed.; Methuen & Co., Ltd.: London, 1969.

Scheme II



4, hydrate  5, keto  6

9  8, enol  7, keto



**Figure 1.** Initial absorbances of OPA in aqueous 0.100 M KCl at 25.0 °C at 260 nm. (a) $1.00 \times 10^{-4}$ M OPA; (b) $5.00 \times 10^{-4}$ M OPA, $5.00 \times 10^{-4}$ M Zn(II).

significant, resulting in changes in hydrogen ion concentrations that were too rapid to allow for the collection of accurate data. In low pH regions, the collection of kinetic data is limited by weak absorbance values of OPA–metal ion systems under the experimental conditions employed. These weak absorbance values are attributed to a large degree of uncomplexed substrate. The absorption by the decarboxylation product, AKBA, was found to be negligible at 260 nm on the basis of measured ultraviolet spectra of $1.00 \times 10^{-4}$ M AKBA and $1.00 \times 10^{-4}$ M metal ion (Zn$^{2+}$, Al$^{3+}$, Cu$^{2+}$) systems at various hydrogen ion concentrations.

**Computations.** Computer programs were developed to calculate the species distribution of metal chelates, free ligand, free metal ion, and metal hydroxide species in solution and to determine the values of the first-order rate constants of decarboxylation of the metal chelates. The species distributions of OPA with Al(III), Zn(II), and Cu(II) were determined with the program SPECIES developed by Dr. R. J. Motekaitis.[30] The values of the proton association and metal ion stability constants of OPA employed in the calculation were reported by Kubala and Martell.[27] The values of the metal ion–hydroxide ion stability constants were those reported by Martell and Smith.[31]

## Results and Discussion

**Ultraviolet Spectra of OPA–Zn(II).** Rapid scans between 200 and 350 nm taken 30 s after the time of mixing on $5.0 \times 10^{-4}$ M solutions of 2-oxalopropionic acid in 0.10 M aqueous KCl at 25.0 °C in the presence of an equivalent amount of Zn(II) as a function of pH reveal that the maximum absorption shifts from 250 nm at pH $\sim$2 to 260 nm at pH $\sim$6. The same absorption shift is seen in the absence of zinc ion, but the optical density is much lower. The pH dependence of the optical density of OPA–Zn(II) solutions is similar to that observed for oxaloacetic acid.[9,15,17] The increase in absorption that accompanies an increase in pH for aqueous OPA has been described by Kubala and Martell[27] in terms

(30) Motekaitis, R. J.; Martell, A. E., to be published.
(31) Martell, A. E.; Smith, R. M. "Critical Stability Constants"; Plenum Press: New York, 1977; Vol. 3.

Table I. Initial Absorbances ($A_I$) and Rate Constants ($k_{obsd}$ and $k_{corr}$) for the Decarboxylation of OPA in the Presence of Metal Ions (25.0 °C, $\mu = 0.1$ M KCl)

| | Zn(II)[a] | | | Al(II)[b] | | | Cu(II)[c] | | |
|---|---|---|---|---|---|---|---|---|---|
| pH | $A_I$ | $k_{obsd}$, $10^3$ s$^{-1}$ | $k_{corr}$, $10^3$ s$^{-1}$ | $A_I$ | $k_{obsd}$, $10^3$ s$^{-1}$ | $k_{corr}$, $10^3$ s$^{-1}$ | $A_I$ | $k_{obsd}$, $10^3$ s$^{-1}$ | $k_{corr}$, $10^3$ s$^{-1}$ |
| 1.5 | | | | 0.12 | 0.92 | 0.86 | | | |
| 1.7 | | | | 0.21 | 1.59 | 1.53 | 0.14 | 1.87 | 1.80 |
| 1.8 | | | | 0.27 | 2.07 | 2.01 | | | |
| 1.9 | | | | | | | 0.24 | 3.07 | 3.00 |
| 2.0 | | | | 0.40 | 3.04 | 2.97 | 0.29 | 3.75 | 3.68 |
| 2.2 | | | | 0.53 | 4.10 | 4.05 | | | |
| 2.3 | 0.06 | 0.24 | 0.13 | 0.59 | 4.63 | 4.56 | 0.46 | 5.76 | 5.69 |
| 2.5 | 0.08 | 0.33 | 0.22 | 0.69 | 5.63 | 5.55 | 0.56 | 6.91 | 6.85 |
| 2.6 | | | | | | | 0.61 | 7.41 | 7.35 |
| 2.7 | 0.12 | 0.45 | 0.33 | 0.78 | 6.55 | 6.49 | | | |
| 2.9 | 0.15 | 0.67 | 0.55 | | | | 0.71 | 8.63 | 8.56 |
| 3.2 | 0.25 | 1.12 | 1.00 | 0.89 | 8.47 | 8.45 | | | |
| 3.33 | 0.30 | 1.34 | 1.22 | | | | 0.81 | 9.71 | 9.68 |
| 3.5 | | | | | | | 0.84 | 10.08 | 10.05 |
| 3.6 | 0.45 | 2.11 | 2.00 | 0.92 | 9.52 | 9.49 | | | |
| 3.8 | 0.61 | 2.72 | 2.62 | 0.93 | 9.92 | 9.87 | | | |
| 3.9 | | | | | | | 0.88 | 10.58 | 10.56 |
| 4.1 | 0.83 | 3.67 | 3.58 | 0.93 | 10.34 | 10.33 | | | |
| 4.2 | | | | | | | 0.89 | 10.79 | 10.78 |
| 4.4 | 1.02 | 3.96 | 3.88 | | | | | | |
| 4.5 | | | | 0.90 | 10.66 | 10.65 | 0.89 | 10.93 | 10.92 |
| 4.6 | 1.12 | 4.87 | 4.80 | | | | 0.90 | 10.95 | 10.94 |
| 4.8 | | | | 0.86 | 10.89 | 10.88 | | | |
| 4.9 | 1.23 | 5.03 | 4.96 | | | | 0.90 | 11.01 | 11.00 |
| 5.1 | | | | 0.80 | 11.22 | 11.22 | | | |
| 5.4 | 1.31 | 5.18 | 5.12 | | | | | | |

[a] 260 nm; equimolar concentrations, $5.00 \times 10^{-4}$ M.  [b] 260 nm; equimolar concentrations, $1.000 \times 10^{-4}$ M.  [c] 290 nm, equimolar concentrations, $1.000 \times 10^{-4}$ M.

of the species in Scheme II and the corresponding equilibrium constants expressed by eq 1–5.

$$K_H = [5]/[4] \tag{1}$$

$$K_1 = [H_2L]/([HL^-][H^+]) \tag{2}$$

$$K_2 = [HL^-]/([L^{2-}][H^+]) \tag{3}$$

$$K_E = [7]/[8] \tag{4}$$

$$K_3 = [L^{2-}]/([H_{-1}L^{3-}][H^+]) \tag{5}$$

The enhancement of optical density in the presence of zinc, shown in Figure 1, can be explained by a modified equilibrium argument, proposed by Bamann and Sethi[15] for the similar behavior in OAA–metal ion systems. The enhanced intensity of the absorption maximum of OPA in the presence of Zn(II) occurs because zinc ions promote enolization of the substrate since the hydroxyl oxygens have stronger coordination tendencies than carbonyl oxygens. This results in larger total concentrations of enol dianion (free and coordinated), which has a much larger extinction coefficient than that of the keto dianion ($14.7 \times 10^3$ and 360 M$^{-1}$ cm$^{-1}$, respectively).[27] The equilibria between OPA and Zn(II) elucidated by Kubala and Martell[27] are shown in Scheme III.

Table I lists the initial absorbances at 260 nm for $5.0 \times 10^{-4}$ M solutions of 2-oxalopropionic acid ($\mu = 0.100$ M KCl, $t$ 25.0 °C, $1.0 \times 10^{-4}$ M OPA) as a function of pH in the absence and in the presence of an equimolar concentration of Zn(II) ion. It is possible to calculate the concentrations of species present at a given pH since the proton associaton constants, $K_H$ and $K_E$, and metal ion stability constants have been determined previously.[27] Also, since the extinction coefficients of the substrate species are known,[27] an extinction coefficient for the metal chelate may be calculated with eq 6, where $A_T^{pH}$ is the total absorbance at a given

$$A_T^{pH} = l\sum_{i=4}^{10} \epsilon_i c_i \tag{6}$$

pH, $l$ is the cell path length, $\epsilon_i$ are the extinction coefficients corresponding to the species shown in Schemes II and III, and

Scheme III
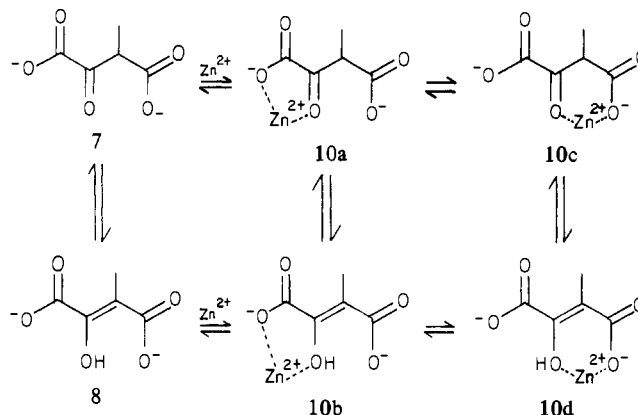


$c_i$ are the respective concentrations at a specified pH. Since calculations reveal that species **9** is not present in significant amounts in solution and **4** and **5** have negligible absorbances under the experimental conditions employed, the total absorbance equation reduces to (7), where the values of $\epsilon_6$, $\epsilon_7$, and $\epsilon_8$ are 88,

$$A_T^{pH} ; l(\epsilon_6 c_6 + \epsilon_7 c_7 + \epsilon_8 c_8 + \epsilon_{10} c_{10}) \tag{7}$$

360, and $14.7 \times 10^3$ M$^{-1}$ cm$^{-1}$, respectively. The value determined for $\epsilon_{10}$ is $(6.37 \pm 0.15) \times 10^3$ M$^{-1}$ cm$^{-1}$.

Since Zn(II) does not appreciably affect the wavelength of maximum absorption, it is reasoned that the $\pi$–$\pi^*$ transition of the enol dianion is not altered, and it is assumed the allowability of the transition is not significantly changed. Therefore, a simple first-order assumption is that the extinction coefficient of the keto and enol forms in the metal ion–substrate complex are not appreciably affected. It is recognized that the value of the extinction coefficient cannot be predicted from the wavelength of the transition, nor can the change in absorption magnitude be predicted based upon the shift in wavelength, but since the system appears unaltered it is assumed energy levels and symmetry factors are basically unchanged, resulting in very little change in the
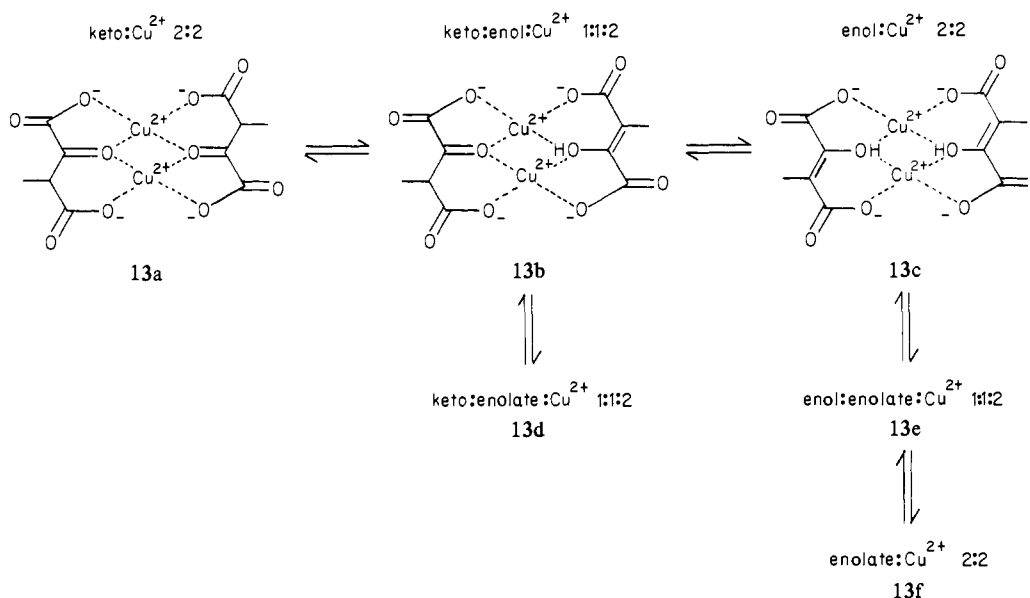
Scheme IV

keto:Cu$^{2+}$ 2:2          keto:enol:Cu$^{2+}$ 1:1:2          enol:Cu$^{2+}$ 2:2

**13a**                **13b**                **13c**

keto:enolate:Cu$^{2+}$ 1:1:2          enol:enolate:Cu$^{2+}$ 1:1:2

**13d**                **13e**

enolate:Cu$^{2+}$ 2:2

**13f**

Table II. Percent Enol Form in the Metal Chelates and Microscopic Rate Constants ($k_{ML}$, $k^K_{ML}$, $k_{ML_2}$, $k^K_{ML_2}$) for the Decarboxylation of OPA in the Presence of Metal Ions (25.0 °C, $\mu$ = 0.1 M KCl)

| rate constant $\times 10^3$ s$^{-1}$ | Zn(II) | % enol | Al(III) | % enol | Cu(II) | % enol |
|---|---|---|---|---|---|---|
| $k_{ML}$ | 18.2 | 42 | 9.51 | 88 | 21.0 | |
| $k^K_{ML}$ | 31 | | 79 | | | |
| $k_{ML_2}$ | | | 33.5 | 23 | | |
| $k^K_{ML_2}$ | | | 43 | | | |

extinction coefficients of the enol and keto forms upon chelation with the non-transition-metal ion Zn(II). On this basis, the percent of chelates of the keto (**10a, 10c**) and enol (**10b, 10d**) forms may be calculated with eq 8 and 9, where $c_{10,K}$ and $c_{10,E}$ are the con-

$$\epsilon_{10}c_{10} = \epsilon_{10,K}c_{10,K} + \epsilon_{10,E}c_{10,E} \qquad (8)$$

$$c_{10} = c_{10,K} + c_{10,E} \qquad (9)$$

centrations of keto and enol chelates of OPA, respectively, and $\epsilon_{10,K}$ and $\epsilon_{10,E}$ are 360 and 14 700 M$^{-1}$ cm$^{-1}$, respectively. The solution of these simultaneous equations results in values that indicate that 42% of the metal chelate is in the enol form (Table II).

Tate, Grzybowski, and Datta[32] have reported that chelate formation with Mg(II) complexes increases the enol content of OAA$^{2-}$ from 14% to 24%. Covey and Leussing[9] reported that Zn(II) further increases the enol proportion and explained this by invoking the softer Lewis acidity of Zn(II) relative to Mg(II). Also, Covey and Leussing[9] used a large excess of metal ion resulting in the formation of a binuclear enolate (**11**). The existence
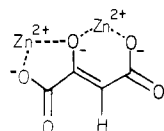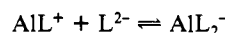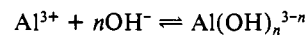
**11**, binuclear Zn(II)–OAA chelate

of such a species would certainly account for the large percent of enolate that they reported. Ultraviolet data obtained in the present study indicate that this type of complex species is not present in significant amounts in the OPA–Zn(II) system, since the absorbance maximum for the enolate species of OPA was measured[27] at 275 nm and the longest wavelength obtained in the

current investigation occurs at 260 nm. This conclusion is supported by previous potentiometric studies[27] that show that Zn-(II)–enolate is not present under the experimental conditions employed in this investigation.
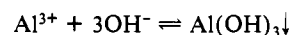
**Ultraviolet Spectra of OPA–Al(III) Solutions.** Rapid scans of 1.00 × 10$^{-4}$ M solutions of 2-oxalopropionic acid in 0.100 M aqueous KCl at 25.0 °C in the presence of an equimolar amount of Al(III) in the pH range 2–5 show shifts in the absorption maximum similar to those seen when Zn(II) was present, but the apparent extinction coefficient of the solution is larger. There also is a pH dependence of the optical density at 260 nm in OPA–Al(III) solutions, with a maximum intensity occurring around pH 4 and an observable decrease in intensity between pH 4 and 5. Above pH 5 a precipitate is observed. This absorption behavior of OPA–Al(III) systems patterns the OPA–Zn(II) systems and may be explained with reaction schemes similar to Schemes I and II, with the inclusion of the following additional equilibria.

$$AlL^+ + L^{2-} \rightleftharpoons AlL_2^-$$

$$K_2 = \frac{[AlL_2^-]}{[AlL^+][L^{2-}]} \qquad (10)$$

$$Al^{3+} + nOH^- \rightleftharpoons Al(OH)_n^{3-n}$$

$$K_n^{OH} = \frac{[Al(OH)_n^{3-n}]}{[Al^{3+}][OH^-]^n} \qquad (11)$$

$$Al^{3+} + 3OH^- \rightleftharpoons Al(OH)_3\downarrow$$

$$K_{sp} = [Al^{3+}][OH^-]^3 \qquad (12)$$

The decrease in optical density above pH 4 is attributed to the decrease in metal chelate concentration, as the result of the formation of soluble hydroxo metal ion complexes. The precipitate above pH 5 is Al(OH)$_3$. This explanation is supported by the species distribution curves shown in Figure 2, which were calculated from the proton association constants and the metal ion stability constants described above.

Initial absorbance measured at 260 nm for 1.00 × 10$^{-4}$ M solutions of OPA ($\mu$ = 0.100 M KCl, $t$ 25.0 °C) in the presence of an equivalent amount of Al(III) ion are presented in Table I and plotted in Figure 3. The method described for the calculation of the extinction coefficient for the ML species in the OPA–Zn(II) system was employed to determine the extinction coefficients of the 1:1 and 1:2 Al(III)–substrate chelates, $\epsilon_{10}$ and $\epsilon_{12}$, respectively. It is noted that not all of the initial absorbance data are employed in this calculation. In the weakly acidic regions the observed rate

(32) Tate, S. S.; Grzybowski, A. K.; Datta, S. P. *J. Chem. Soc.* **1964**, 1372, 1381.
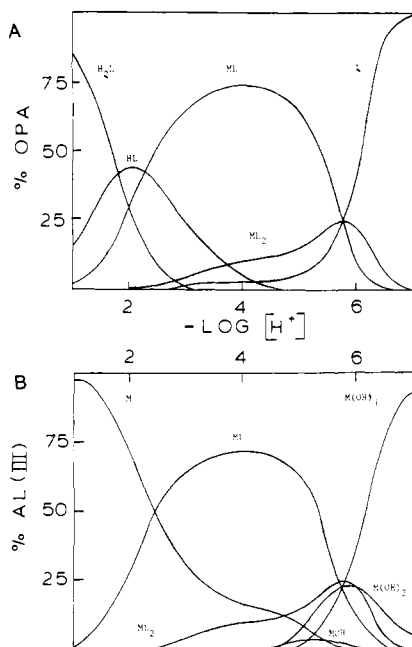
6606   *J. Am. Chem. Soc., Vol. 104, No. 24, 1982*

*Kubala and Martell*

**Figure 2.** Distribution of species present in equimolar Al(III)–OPA solutions at $1.00 \times 10^{-4}$ M total concentrations of ligand and metal ion, $\mu = 0.100$ KCl at 25.0 °C: (A) ligand distribution; (B) metal ion distribution.
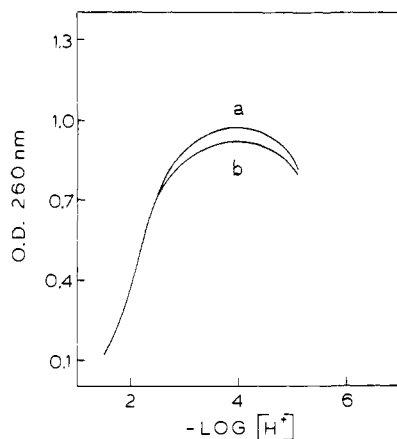


**Figure 3.** Optical densities at 260 nm of $1.0 \times 10^{-4}$ M OPA in the presence of an equimolar amount of Al(III) at 25.0 °C; $\mu = 0.100$ M KCl. (a) Calculated initial absorbance; (b) observed initial absorbance.

of decarboxylation is sufficiently high that appreciable decarboxylation and a detectable decrease in substrate concentration occurs by the time ($\sim$30 s) that initial absorbance is measured. Raghavan and Leussing[10] also detected a short burst of decarboxylation in the OAA systems in which there is almost 100% chelate formation and explained this observation by pointing out that the substrate is initially in the decarboxylation-active keto form when complexation first occurs. The metal chelate of the keto form of the ligand may then decarboxylate or enolize. If the decarboxylation rate constant is sufficiently large, significant amounts of substrate may decompose before keto $\rightleftharpoons$ enol equilibrium is achieved. Termination of the short burst of decarboxylation could also be the result of an additional equilibrium that involves the formation of a dimer by condensation of the methylene group of one $\beta$-carboxy $\alpha$-keto acid molecule to the carbonyl group of another. Dimerization resulting from aldol condensation has been reported to occur quite readily for AKBA in the presence of Zn(II) by Abbott and Martell.[33]

In the present studies below pH 2.5, the amount of complexed ligand is less than 50% and the observed decarboxylation rate

constant is low enough that practically all of the substrate is present when the initial optical density measurement is made. Therefore, in the pH range 1–2.5 the initial abosrbance measurements are used in the extinction coefficient calculations for the 1:1 and 1:2 metal–ligand complexes. The total absorbance for the OPA–Al(III) system is expressed by

$$A_T^{pH} = l(\epsilon_6 c_6 + \epsilon_7 c_7 + \epsilon_8 c_8 + \epsilon_{10} c_{10} + \epsilon_{12} c_{12}) \quad (13)$$

where $\epsilon_{12}$ and $c_{12}$ are the extinction coefficient and concentration of the 1:2 aluminum(III)–substrate complex species (not shown), which reduces to

$$B/c_{10} = \epsilon_{10} + \epsilon_{12} c_{12}/c_{10} \quad (14)$$

with

$$B = A_T/l - \epsilon_6 c_6 - \epsilon_7 c_7 - \epsilon_8 c_8$$

A plot of $B/c_{10}$ vs. $c_{12}/c_{10}$ gave a straight line, and a linear least-squares fit yielded values of $13.1 \times 10^3$ (intercept) and $5.00 \times 10^3$ M$^{-1}$ cm$^{-1}$ (slope) for the extinction coefficients of the AlL$^+$ and AlL$_2^-$ species, respectively. A plot of calculated initial absorption based upon known extinction coefficients and concentrations for this system is given in Figure 3. Above pH 3 there is a difference between calculated and observed initial absorbance curves. This difference is the consequence of the short burst of decarboxylation that occurs after mixing and before equilibrium is reached, as described above.

Since the presence of Al(III) does not result in an appreciable shift in the absorption maximum, a hypothesis similar to that made for the OPA–Zn(II) system, that the extinction coefficients of the keto dianion and enol dianion in the metal ion–substrate complexes are essentially equivalent to those of the corresponding uncoordinated ligand species, was employed. Also, since previous potentiometric investigations[27] show no significant amount of free or coordinated enolate to be present, the absorption data were used to calculate the percent enol form of the substrate in the ML and ML$_2$ species. The values obtained are 88% and 23% in the ML and ML$_2$ species, respectively. The high percentage of enol for the 1:1 chelate is reasonable because of the high charge of the metal ion and the large metal ion stability constant (log $K_{ML}$ = 6.61).[27] The decrease in percent enol in going from the ML to the ML$_2$ species is attributed to the lower effective positive charge experienced by the coordinated substrate dianion in the 1:2 metal chelate.

**Ultraviolet Spectra of OPA–Cu(II).** Initial scans of acidic solutions of $1.0 \times 10^{-4}$ M 2-oxalopropionic acid ($\mu = 0.100$ M KCl, $t$ 25.0 °C) with equimolar amounts of Cu(II) were obtained 30 s after the time of mixing. These results and the rate constants obtained are given in Table I. The typical pH dependence of optical density described above for Zn(II) systems was observed, but the absorption maximum was located at 290 nm in acidic aqueous solutions. This shift to a longer wavelength in the Cu-(II)–OPA system may be attributed to either of two possible phenomena: either Cu(II) enhances the concentration of the enolate form or the d orbitals of the cupric ion interact with the conjugated $\pi$ system of the ligand. Either possibility would account for the observed spectral shift. A previous potentiometric investigation[27] revealed that no enolate species, free or coordinated, exist under the experimental conditions employed and that the equilibria presented in Schemes I and II apply to this system, along with the following additional equilibrium:

$$2CuL \rightleftharpoons Cu_2L_2$$
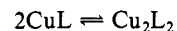
Since the previous equlibrium studies show that no free or coordinated enolate is present, it is proposed that the observed shift in the ultraviolet spectra is the result of weak d$\pi$–p$\pi$ interaction.

In view of the interaction between Cu(II) d orbitals and the OPA$^{2-}$ $\pi$ system, the $\pi$–$\pi^*$ transition is affected and the assumption made earlier in the Zn(II) and Al(III) systems that the extinction coefficients of the enol and keto dianion species in their free and chelated forms are equivalent is not expected to hold. This means that estimates of percent enol formation in the ML and M$_2$L$_2$ species cannot be accurately made. Nevertheless,

(33) Abbott, E. H.; Martell, A. E. *J. Am. Chem. Soc.* **1969**, *91*, 6931.
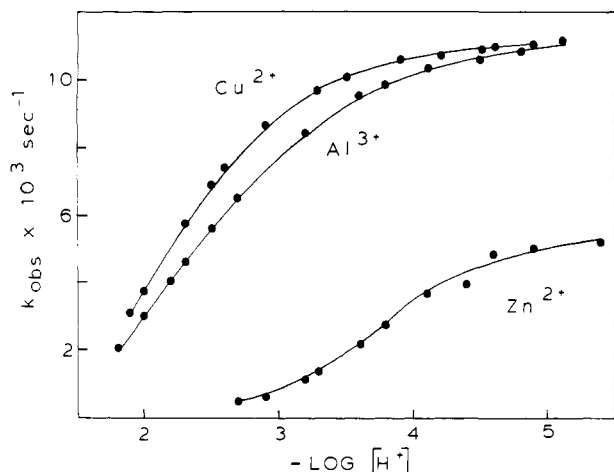
**Figure 4.** Rate constant–pH profile of the metal ion catalyzed decarboxylation of 2-oxalopropionic acid in the presence of an equimolar amount of metal ion in aqueous 0.100 M KCl at 25.0 °C. Cu(II) = 1.00 × 10⁻⁴ M, Al(III) = 1.00 × 10⁻⁴ M, and Zn(II) = 5.00 × 10⁻⁴ M.

observed extinction coefficients for the ML and $M_2L_2$ species, $\epsilon_{10}$ and $\epsilon_{13}$, respectively, may be calculated from the optical density data at 290 nm. The calculation of these extinction coefficients is simplified because under the experimental conditions employed none of the free ligand species have an appreciable absorbance at this wavelength. At 290 nm, the equation for total absorbance at a given pH is

$$A_T^{pH} = (\epsilon_{10}c_{10} + \epsilon_{13}c_{13})l \qquad (15)$$

where $c_{13}$ is the concentration of the $M_2L_2$ species. Only the initial absorbances from pH 1.5 to 2.7 were used because this is a region where the ligand is not totally chelated and in which the short burst of decarboxylation mentioned above is avoided. That is, the observed rate constant is small enough to avoid measurable decarboxylation before the first absorbance measurement. The total absorbance equation may be rearranged to

$$A_T^{pH}/lc_{10} = \epsilon_{10} + \epsilon_{13}c_{13}/c_{10} \qquad (16)$$

A plot of $A_T^{pH}/lc_{10}$ vs. $c_{13}/c_{10}$ yields a straight line. Linear least-squares treatment yields values of 4.64 × 10³ and 16.1 × 10³ M⁻¹ cm⁻¹ for $\epsilon_{13}$ and $\epsilon_{10}$, respectively. It is notable that the extinction coefficient of the ML species is greater than that of the enol species, an observation that supports the interpretation that there is interaction between the Cu(II) d orbitals and the π system of OPA.

A comparison of pH–absorbance plots for calculated and measured absorbance (not shown) demonstrates that considerable decarboxylation occurs above pH 3.8 before the initial absorbance is measured. At this point (pH 3.8), less than 50% of the substrate is in a noncomplexed form.

**Kinetics of Decarboxylation of OPA–Zn(II).** Kinetic data on 5.0 × 10⁻⁴ M OPA solutions in aqueous 0.100 M KCl in the presence of equimolar concentrations of zinc(II) ion (Table I) were obtained by monitoring the initial decrease in absorbance at 260 nm. The kinetic data may be fitted to eq 17, where $A$ is the

$$\ln (A/A_0) = -k_{obsd}t \qquad (17)$$

absorbance at a given time, $t$, $A_0$ is the calculated initial absorbance of OPA, and $k_{obsd}$ is the initial observed rate constant for decarboxylation. A plot of ln $(A/A_0)$ vs. $t$ yielded a straight line having a slope equivalent to $-k_{obsd}$. An advantage of this plot is that it reveals whether or not measurable decarboxylation took place before the initial absorbance reading is made since the first data point is located on the time axis if no appreciable decarboxylation had occurred.

Figure 4 shows a pH–rate constant profile of the observed decarboxylation rate constant obtained in the presence of zinc(II) ion while Figure 5 shows the species distribution of a 1:1 Zn-(II)–OPA system at concentrations employed in the kinetic ex-
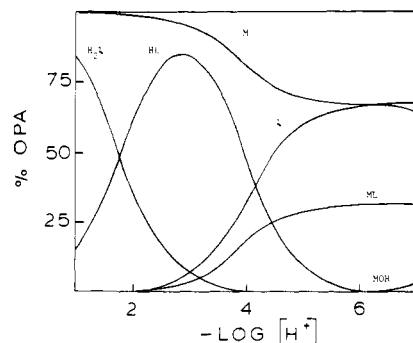


**Figure 5.** Ligand species distribution of equimolar Zn(II) and OPA at 5.00 × 10⁻⁴ M total ligand and metal ion concentrations with $\mu$ = 0.10 M KCl at 25.0 °C. 2-Oxalopropionic acid = $H_2L$.

periments. A visual inspection of these two figures demonstrates that rate constant enhancement accompanies increased metal chelate formation.

The observed rate constant at any given pH may be described by eq 18, where $k_i$ are the rate constants of the species denoted

$$k_{obsd} = k_{H_2L}\alpha_{H_2L} + k_{HL}\alpha_{HL} + k_L\alpha_L + k_{ML}\alpha_{ML} \qquad (18)$$

by the subscript and $\alpha_i$ are fractions of total OPA for the individual species in solution. The observed rate constant may be corrected for the spontaneous decarboxylation of the various free ligand species with rate constants published previously:

$$k_{corr} = k_{obsd} - k_{H_2L}\alpha_{H_2L} - k_{HL}\alpha_{HL} - k_L\alpha_L = k_{ML}\alpha_{ML} \qquad (19)$$

where the values of $k_{H_2L}$, $k_{HL}$, and $k_L$ are 1.67 × 10⁻⁵ s⁻¹, 13.5 × 10⁻⁵ s⁻¹, and 7.75 × 10⁻⁵ s⁻¹, respectively,[19] and calculated values of $k_{corr}$ are listed in Table I. These rate constants were determined in deuterium oxide but will serve as a first-order correction on $k_{obsd}$ since $D_2O$ shifts the maximum point of decarboxylation rate to slightly higher pD but has very little effect on the magnitude of the rate maximum.[4] It is assumed that the main reason for this behavior is that the deuterium oxide medium alters the $pK_a$s of OPA and therefore changes the pH (pD) dependence only slightly while the deuterium oxide medium has little or no effect on the decarboxylation rates of the neutral acid, mono-, or dianion substrate species.[4]

A plot of $k_{corr}$ vs. $\alpha_{ML}$ yielded a straight line with slope $k_{ML}$. A linear least-squares treatment of this correlation gave 18.2 × 10⁻³ s⁻¹ as the value of $k_{ML}$. This rate constant can be expressed in terms of the rate constants for the metal complexes of the enol (**1b, 2b**) and keto (**1a, 2a**) forms of the substrate in accordance with eq 20, where $k^K_{ML}$ and $k^E_{ML}$ are rate constants for the keto

$$k_{ML} = k^K_{ML}\alpha_K + k^E_{ML}\alpha_E \qquad (20)$$

and enol metal chelates, respectively, and $\alpha_K$ and $\alpha_E$ are the corresponding fractions of these metal ion–substrate complexes in solution. It has been shown that the most rapid pathway for the spontaneous decarboxylation of OPA occurs through the formation of the monanion **5b**, whereas the diprotonated and the



5b
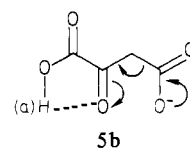
fully ionized forms tend to decompose at slower rates.[19] The generally accepted explanation for this experimental observation is that the carboxyl group must be negatively charged for the electron shift required for decarboxylation to occur and that the existence of the hydrogen bond between the oxalyl carboxyl and the α-carbonyl assists in the electron shift. When coordinated metal ions occupy the position held by the hydrogen ion labeled (a) in **5b**, as indicated by **1a** in Scheme I, further increases in rate are observed because the charge of the metal ion facilitates the required shift of electrons. The initial rise in rate with increasing pH corresponds to increased metal ion coordination. On the other

hand the enol complex, **1b**, is considered inactive since the electron shift necessary for decarboxylation cannot occur in this complex. Thus eq 3 simplifies to

$$k_{ML} = k^K{}_{ML}\alpha_K \qquad (21)$$

with $\alpha_K$ estimated at 0.58 from a previous calculation based upon the initial absorbance data. A simple computation yields a value of $31 \times 10^{-3}$ s$^{-1}$ for $k^K{}_{ML}$. Raghavan and Leussing[10] have reported a rate constant for decarboxylation of Zn(II)–OAA keto of 47 $\times 10^{-3}$ s$^{-1}$. The values of $k_{ML}$ and $k^K{}_{ML}$ are presented in Table II along with the Al(III) and Cu(II) rate constants for comparison.

The results for OPA determined here differ somewhat from those reported for OAA by Munakata et al.[14] and Covey and Leussing.[9] These differences may be the result of either dissimilar experimental conditions, an inherent difference between these two substrates, or a combination of both. Munakata et al.[14] reported that a maximum in the observed decarboxylation rate constant of OAA in the presence of Zn(II) occurs around pH 5. No such maximum was found in the OPA–Zn(II) system. This may be explained by the different metal-ion stability constants of the Zn(II) chelates. The formation constant of the Zn(II)–OAA chelate reported by Covey and Leussing[9] is $10^{2.41}$ in 0.10 M KCl. This value is approximately 0.7 log unit smaller than the formation constant reported for Zn(II)–OPA, $10^{3.13}$. For OAA, with a lower formation constant of the Zn(II) complex relative to that of the OPA analogue, it is expected that the hydroxo–metal ion concentration becomes significant at slightly lower pHs than is the case of the present study of OPA. In the Zn(II)–OPA system the monohydroxo species first appears around pH 6 and increases in concentration as the pH is increased. It is likely that in the Munakata study metal ion hydrolysis significantly decreases the concentration of catalytic metal ion and thereby decreases the rate of decarboxylation.

The large excess of metal ion used by Covey and Leussing[9] results in the formation of an inactive binuclear complex ($M_2L$). Above pH 4.0 this inactive species begins to increase in concentration, reducing the concentration of the active metal chelate and resulting in the decrease in the decarboxylation rate. As previously stated for the OPA–Zn(II) system, no such binuclear enolate species is detected under the experimental conditions employed in this investigation below pH 7.

**Kinetics of Decarboxylation of OPA–Al(III).** The rates of decrease in absorbance at 260 nm of $1.000 \times 10^{-4}$ M OPA in the presence of an equimolar concentration of aluminum(III) in aqueous 0.100 M KCl were treated in the manner described for the Zn(II) system, and the values of $k_{obsd}$ obtained are listed in Table I and are plotted in Figure 4. The species distribution for this system, Figure 2, shows that the reactive ML species reaches its maximum concentration at approximately pH 4. On the other hand, $k_{obsd}$ does not have a maximum at pH 4 but continues to increase until at least pH 5. This behavior is interpreted in terms of the formation of a second reactive species, the $ML_2$ chelate containing two substrate ligands coordinated through carboxylated and carbonyl oxygen donors. With the inclusion of this species in the decarboxylation process, the equation for $k_{corr}$ becomes

$$k_{corr} = k_{ML}\alpha_{ML} + k_{ML_2}\alpha_{ML_2} \qquad (22)$$

and the calculated values of $k_{corr}$ are listed in Table I. A plot of $k_{corr}/\alpha_{ML}$ vs. $\alpha_{ML_2}/\alpha_{ML}$ yielded a straight line with $9.51 \times 10^{-3}$ s$^{-1}$ as the intercept ($k_{ML}$) and a slope ($k_{ML_2}$) of $33.5 \times 10^{-3}$ s$^{-1}$. It is seen here that the rate constant of the $ML_2$ species is several times larger than that of the ML species, a result which at first was not expected since the effective positive charge of the metal ion is diminished in the complex having 2 mol of ligand per metal ion. However, the percent keto form in the 2:1 complex is much larger than in the 1:1. When a decarboxylation rate constant is calculated with eq 4 for the keto form in these metal complexes, the the values 79 $\times 10^{-3}$ s$^{-1}$ and 43 $\times 10^{-3}$ s$^{-1}$ for $k^K{}_{ML}$ and $k^K{}_{ML_2}$, respectively, were obtained. Thus in the active keto complexes the metal ion exerts a significantly higher catalytic effect in the 1:1 complex relative to that of the 1:2 complex. An important concept is demonstrated by comparing the values of $k_{ML}$, $k_{ML_2}$,
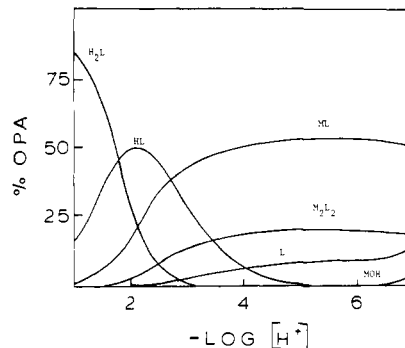


**Figure 6.** The species distributions in a solution having a 1:1 molar ratio of OPA to Cu(II); $[Cu^{2+}]_T = [OPA] = 1.00 \times 10^{-4}$ M at 25.0 °C in 0.100 M KCl solutions.

$k^K{}_{ML}$, and $k^K{}_{ML_2}$ in the zinc and aluminum ion studies listed in Table II. The greater the stability constant and the more positive the metal ion, the stronger the catalytic effect in the keto form of the chelate at the microscopic level. However, increased complex stability coupled with the larger effective positive charge of the metal ion converts relatively larger fractions of substrate to the inactive enol forms. The observed rate constant of decarboxylation is therefore the result of a balance between these factors, and overall higher metal ion–ligand affinity may easily result in a lowering of the catalytic effect of the metal ion on the decarboxylation process.

**Kinetics of Decarboxylation of OPA–Cu(II).** The mathematical treatment described above was used to calculate $k_{obsd}$ values for the kinetic data obtained by monitoring the decrease in ultraviolet absorbance at 290 nm of $1.00 \times 10^{-4}$ M OPA in the presence of $1.00 \times 10^{-4}$ M Cu(II). The values of $k_{obsd}$ determined in this manner are presented in Table I and plotted in Figure 4. As seen from the species distribution curves presented in Figure 6, two types of metal ion complexes are formed: the 1:1 copper(II) complexes, ML, and a binuclear dimer, $M_2L_2$. The latter species is involved in keto–enol equilibria analogous to that discussed above for the mononuclear chelates. Since the extinction coefficient of the mononuclear complex is small, it is proposed that a significant portion of the substrate exists in the keto form. The most reasonable explanation for this observation (that **13a** is much more stable than **13c**, **13d**, **13e**, and **13f**) is that the Cu(II) ions in **13a** are four-coordinated and form a neutral complex which has less tendency in acid solution to dissociate one or two protons to form the enolate. Certainly it would appear that **13f** would be the most stable binuclear chelate at high pH.

However, it is not essential that the equilibrium constants for the **13a**–**13f** conversion be known since all forms should be inactive toward decarboxylation. Binding by the Cu(II) ion prevents the lone electron pair of the coordination $\beta$-carboxylate group in **13a**, **13b**, and **13d** from undergoing the electronic shift necessary for decarboxylation. This type of deactivation toward decarboxylation is pH independent (since more highly ionized species are also inactive) but shows metal ion and substrate concentration dependence, since dimerization is favored by high concentrations of both metal ion and ligand. Speck[8] has observed similar behavior in his early work with oxaloacetic acid in the presence of Cu(II).

Since the $M_2L_2$ species is inactive toward decarboxylation, $k_{obsd}$ may be expressed in terms of eq 1. It follows, therefore, that the expression for $k_{corr}$ (eq 2) also applies to this system. A plot of $k_{corr}$ vs. $\alpha_{ML}$ yielded a straight line with a slope ($k_{ML}$) equal to $21.0 \times 10^{-3}$ s$^{-1}$.

Figure 4 demonstrates that in this Cu(II)–OPA system, the observed rate constant for decarboxylation continues to increase in magnitude as the pH increases and does not go through a maximum in the acidic region, whereas Munakata et al.[14] and Raghavan and Leussing[10] have shown enhancement of decarboxylation of OAA with increasing pH in the acidic region followed by inhibition as neutrality is approached. Factors similar to those presented for the Zn(II)–OPA system also seem to apply to copper(II) catalysis. The experimental conditions employed

by Raghavan and Leussing[10] favor the formation of the inactive binuclear Cu(II)–enolate complex, $Cu_2L^+$ (14), as the pH is increased.



**14**
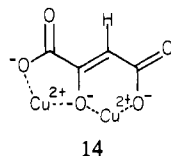
In the work of Munakata et al.[14] the much lower stability constant reported for OAA with Cu(II) (log $K_{ML}$ = 4.1[31]) relative to OPA–Cu(II) interaction reported here (log $K_{ML}$ = 5.82[27]) shows that hydroxide ion competition for the metal ion is much stronger for the OAA system. Thus hydrolysis of the catalytic metal ion would be expected to decrease the concentration of the catalytic OAA complex, ML, as the pH is increased near the neutral pH range.

## Conclusions

Decarboxylation of OPA and other α-keto β-carboxy carboxylic acids is catalyzed by metal ions through the formation of the bidentate metal chelate, ML, involving the α-keto acid functions. A high formation constant of the metal chelate does not necessarily indicate that the rate of decarboxylation will be increased. Although an increase in the magnitude of the stability constant results in greater conversion of the substrate to the chelated form in solution, the tendency for the substrate to be in the inactive enolic form also increases. Competition by hydrogen ion for the substrate and hydroxide ion for the metal ion as well as the tendency to form additional metal chelate species beyond the simple 1:1 metal chelate are important considerations. The 1:2 complex, $ML_2$, and the binuclear chelate, $M_2L$, have characteristic catalytic activities that differ from that of the 1:1 chelate and may also exist partially in the form of the corresponding inactive enolate complexes. Polynuclear complexes such as the dimer $M_2L_2$ may exist in several forms, all of which are relatively inactive.

# Trans 2,6-Bis[(dimethylamino)methyl]phenyl-*N*,*N'*,*C* Complexes of Pd(II) and Pt(II). Crystal Structure of [PtI(MeC₆H₃(CH₂NMe₂)₂-*o*,*o'*)]BF₄: A Cyclohexadienyl Carbonium Ion with a σ-Bonded Metal Substituent

**David M. Grove,[1a] Gerard van Koten,*[1a] Jaap N. Louwen,[1a] Jan G. Noltes,[1b] Anthony L. Spek,[1c] and Henk J. C. Ubbels[1a]**

*Contribution from the Anorganisch Chemisch Laboratorium, J. H. van't Hoff Instituut, University of Amsterdam, 1018 WV Amsterdam, The Netherlands, the Organisch Chemisch Instituut TNO, 3502 JA Utrecht, The Netherlands, and the Laboratorium voor Structuurchemie, Rijksuniversiteit, 3584 CH Utrecht, The Netherlands. Received March 15, 1982*

**Abstract:** The complexes [MBr(C₆H₃(CH₂NMe₂)₂-*o*,*o'*)] (M = Pd, Pt) prepared from the reaction of *cis*-[PtCl₂(SEt₂)₂] or [PdBr₂(c-1,5-C₈H₁₂)] with the anion derived from lithium and *o*,*o'*-(Me₂NCH₂)₂C₆H₃Br contain a divalent metal center with the N donor atoms positioned mutually trans as a result of the geometric restraints of the terdentate monoanionic ligand. Treatment of these complexes with AgBF₄ can be used to generate the species [M(C₆H₃(CH₂NMe₂)₂-*o*,*o'*)(H₂O)]BF₄ (M = Pd, Pt), which are suitable not only as precursors for neutral [MX(C₆H₃(CH₂NMe₂)₂-*o*,*o'*)] (M = Pd, Pt; X = Cl, Br, I) but also for the study of the coordination chemistry induced by the terdentate ligand. The reaction of the cationic platinum analogue with MeI proceeds smoothly to [PtI(MeC₆H₃(CH₂NMe₂)₂-*o*,*o'*)]BF₄ in which the incoming methyl group has ended up transferred to the aryl ring system. A single-crystal X-ray study has revealed the structure of this complex C₁₃H₂₂IN₂PtBF₄: monoclinic space group P2₁/c with unit cell dimensions a = 11.033 (2) Å, b = 11.553 (1) Å, c = 13.915 (3) Å, β = 98.34 (11)°, and Z = 4. The crystal structure was solved by standard Patterson and Fourier techniques. Anisotropic full-matrix least-squares refinement with 3499 observed reflections converged at R = 0.056. The most interesting molecular feature is a "boat" type puckering of the aryl ring which is coordinated in a novel way to the Pt(II) center exhibiting a slightly distorted square-planar coordination. Together with ¹H NMR and CNDO/S calculations on model systems these data suggest that the positive charge of the cation is to a large degree accommodated within the C₆ ring system; i.e., the complex is an example of a stable σ-metal-substituted arenonium ion (cyclohexadienyl cation) analogous to the Wheland intermediates formed during substitution reactions on free aromatic sytems.

## Introduction

The [C₆H₃(CH₂NMe₂)₂-*o*,*o'*] anion is one of the few multidentate ligand systems capable of placing two hard N donor atoms mutually trans across a metal center. By virtue of the rigid coordination of this chelate ligand there remain available a restricted number of specific coordination sites exclusively in a plane perpendicular to that of the ligand. Such a system that can also give enhanced nucleophilic character to a metal offers interesting potential for the study of basic reactions, e.g., electron transfer and oxidative addition (where trans products usually result).

We have in fact used this ligand to isolate many noteworthy complexes, examples being [Pt(C₆H₃(CH₂NMe₂)₂-*o*,*o'*)(μ-(*p*-tolNYNR))HgBrCl] (Y = CH, N)[2] and [Pt(C₆H₃-

(1) (a) University of Amsterdam. (b) Organisch Chemisch Instituut TNO. (c) Rijksuniversiteit.